

Supporting Information

For

γ Radiation Induced Self-Assembly of Fluorescent Molecules into Nanofibers: a Stimuli-responsive Sensing

Ji-Min Han, Na Wu, Brian Wang, Chen Wang, Miao Xu, Xiaomei Yang, Haori Yang, and Ling Zang*

Outline

1.	General methods and materials	S2
2.	Theoretical calculation	S3
3.	Dynamic light scattering measurement	S4
4.	Determination of detection limit	S5
5.	Determination of quantum yield of PI-DPA	S5
6.	Fluorescence spectral change of CHO-TPA upon γ radiation	S6
7.	Fluorescence spectral reversibility test of PI-DPA	S7
8.	Fluorescence spectral comparison of PI-DPA in solutions and thin film	S8
9.	Spectral comparison of PI-DPA in DMSO solution upon HCl addition	S9
10.	Fluorescence spectral change of PI-DMA upon γ radiation	S10
11.	Absorption and fluorescence spectral change of PI-DPA under γ , UV and sun light radiations	S11
12.	^1H NMR spectra of PI-DPA before and after binding with HAC	S12
13.	SEM image of drop cast film of neutral PI-DPA	S13

1. General methods and materials

All the starting materials and organic solvents were purchased from Sigma-Aldrich and used as received unless otherwise stated (e.g., CHCl_3 was further purified before using as solvent for the sensor). The silica gel and TLC plates (Silicycle Ultrapure Silica Gels SIL-5554-7) were purchased from EMD Chemicals Inc. UV-vis absorption spectra were measured on a PerkinElmer Lambda 25 spectrophotometer or Agilent Cary 100. Fluorescence spectra were measured on a PerkinElmer LS 55 spectrophotometer or Agilent Eclipse spectrophotometer. ^1H and ^{13}C NMR spectra were recorded on a Varian Unity 300 MHz Spectrometer at room temperature in appropriate deuterated solvents. All chemical shifts are reported in parts per million (ppm). ESI MS spectra were recorded on a Micromass Quattro II Triple Quadrupole Mass Spectrometer, and the solvent used was methanol. The dynamic light scattering (DLS) measurements were performed on a Malvern Zetasizer Nano ZS (Malvern, Herrenberg, Germany) under the scattering angle of 173° at the wavelength of 360 nm for PI-DPA. Results were reported as the average of five measurements with standard deviations. Bright field and fluorescence optical microscopy images were obtained with Leica DMI4000B inverted microscope equipped with Acton SP-2356 Imaging Spectrograph system and Princeton Instrument Acton PIXIS:400B Digital CCD Camera System for high resolution full spectral recording. Scanning electron microscopy (SEM) measurements were performed with an FEI Nova Nano 630 (FEI Corporation) equipped with a helix detector. All images were captured with the immersion lens in low-vacuum mode (with 0.43 torr water pressure). The electron energy was set to 7kV. In a typical SEM sample preparation, small volume of a PI-DPA solution (with or without addition of HCl) was drop-cast onto a silicon wafer, followed by drying under ambient condition. Samples thus prepared were directly taken for SEM measurement without coating or other treatment. The electrical conductivity (I-V curve) was measured using a two-probe method on a Signatone S-1160 Probe Station combined with an Agilent 4156C Precision Semiconductor Analyzer. A tungsten lamp was used as the white light source, for which the irradiation intensity at the sample surface was 0.25 mW/mm^2 . All the I-V measurements were performed in open air at room temperature. Interdigitated electrodes (20 μm gap, 20 μm width and 1050 μm length of electrode fingers, 10 pairs) patterned on an oxidized silicon wafer (300 nm thick SiO_2) were used for the I-V measurements. Nanofibers or molecules were drop-cast onto the electrodes from the chloroform solutions. The electrode fingers were fabricated with gold atop titanium using sputtering, with thickness of 50 nm and 20 nm, respectively.

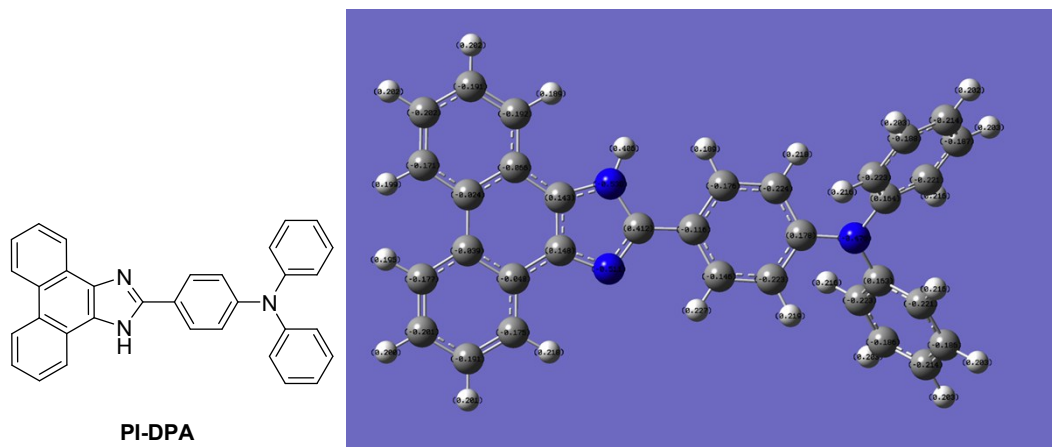
Choice of the solvents: In general, halogenated methanes or ethanes can be used as solvents for radical generation under γ radiation. In this study we chose CHCl_3 as the solvent to characterize the sensor

system mainly because (1) it provides good solubility and strong fluorescence for the sensor molecule, PI-DPA; and (2) it affords high efficiency of HCl production under γ radiation. The chloroform we used was purchased from Sigma-Aldrich. Before using the solvent was further purified to remove the excessive acids and stabilizers, following the method we developed in the previous study (ref. 5h: J. M. Han; M. Xu; B. Wang; N. Wu; X. Yang; H. Yang; B. J. Salter; L. Zang *J. Am. Chem. Soc.* **2014**, *136*, 5090). CH_2Cl_2 was also used as the solvent, and similar sensor response (slightly lower in magnitude) was found in CH_2Cl_2 solution both under γ radiation and acid titration, which is consistent with our previous study (reference above). Halogenated ethanes and other larger alkanes were not used mainly because of their decreased efficiency in production of hydrogen halides.

2. Theoretical calculation

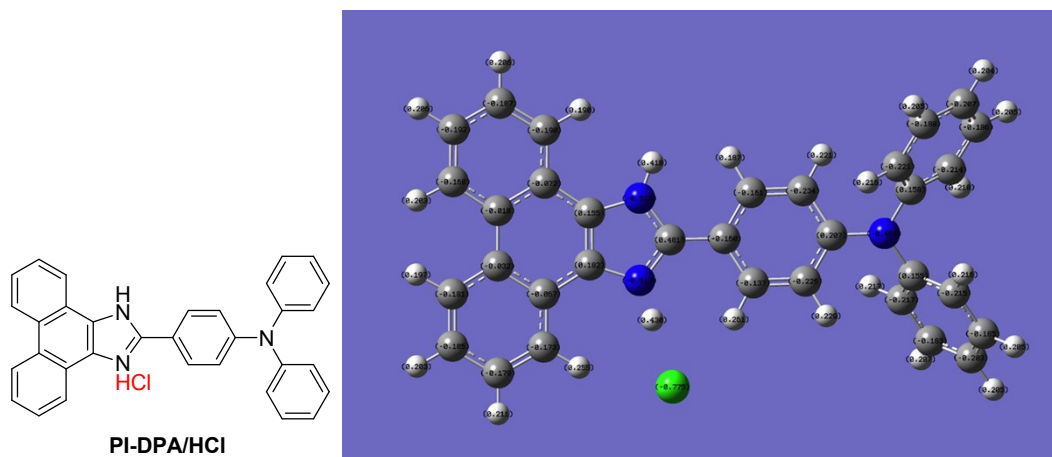
Geometry optimization and energy calculation of molecules were performed with density-functional theory (B3LYP/6-311g**//B3LYP/6-31g*) using Gaussian 09 package.

PI-DPA: td-B3LYP/6-311g**//b3lyp/6-31g*



NImag = 0; LUMO/HOMO: -1.4eV/-5.1eV relative to vacuum level.

PI-DPA/HCl: td-B3LYP/6-311g**//b3lyp/6-31g*



Nimag = 0; LUMO/HOMO: -2.12 eV/-5.56 eV relative to vacuum level.

Figure S1. Calculation results of PI-DPA and the adduct PI-DPA/HCl.

3. Dynamic light scattering measurement

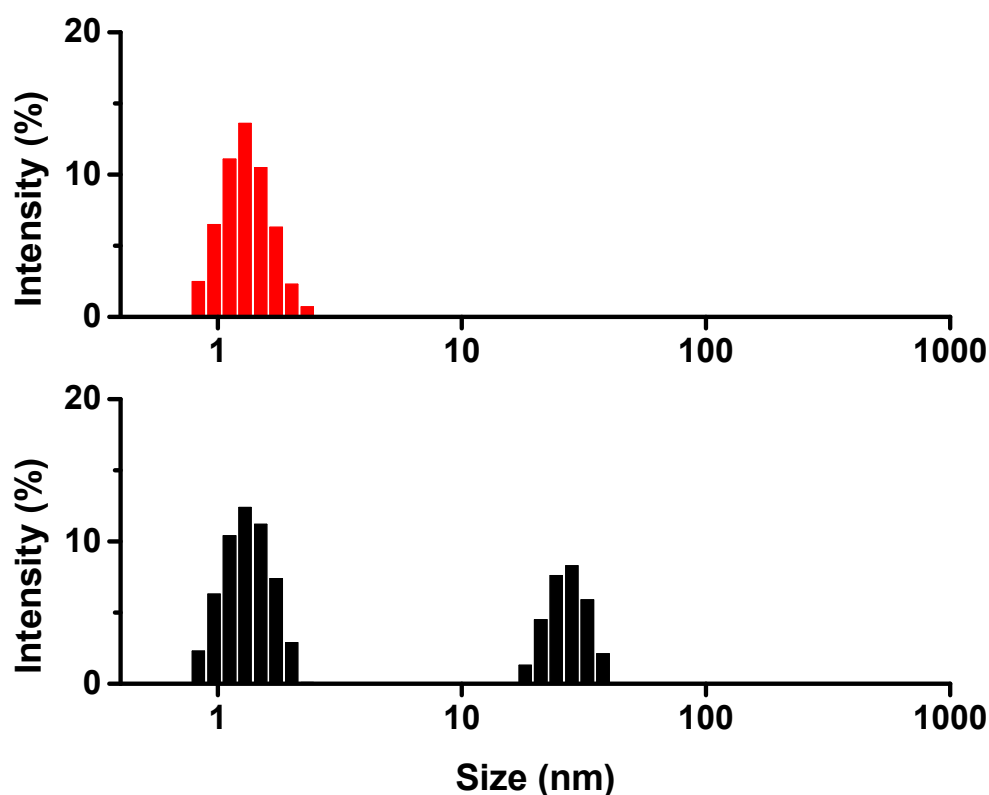


Figure S2. Size distribution by dynamic light scattering (DLS) measured at room temperature for PI-DPA in CHCl_3 solution (1×10^{-5} mol/L) before (upper) and after (below) 5 Gy of γ radiation. Although DLS measurement clearly indicates the formation of molecular aggregate, it does not provide precise measurement of the size and shape of the aggregates, which are actually long nanofibers as revealed by

the SEM imaging (Figure 2 and 4 in main context). DLS is suited for measuring size of spherical particle, but not elongated fibers.

4. Determination of detection limit

(a) Based on absorption measurement shown in Figure 1c

The linear relationship in low dose range (0-2 Gy) can be fitted as

$$y = 0.1235 x + 0.287$$

where y is the absorption measured at 393 nm, and x is the γ radiation dose.

The standard deviation (σ) is defined as the standard error of the absorption measurement, as determined by the baseline measurement of blank sample (measured at 393 nm). If defining three times of the standard deviation as the detectable signal (see ref. 5h and 8), the detection limit can be projected as $3\sigma/\text{slope} = 3 \times 0.00033/0.1235 = 0.008$ Gy.

(b) Based on the fluorescence measurement shown in Figure 1d

The linear relationship in low dose range (0-2 Gy) can be fitted as

$$y = 102.2 x + 109.2$$

where y is the fluorescent intensity measured at 494 nm, and x is γ radiation dose.

The standard deviation (σ) is defined as the standard error of the fluorescence intensity measurement, as determined by the baseline measurement of blank sample (monitored at 494 nm, at fixed instrumentation parameters, e.g., Ex. slit 5 nm, Em. slit 10 nm, PMT voltage 450 V). If defining three times of the standard deviation as the detectable signal (see ref. 5h and 8), the detection limit can be projected as $3\sigma/\text{slope} = 3 \times 0.22/102.2 = 0.006$ Gy.

5. Determination of quantum yield of PI-DPA

The fluorescence quantum yield (Φ_s) of PI-DPA in 1,4-dioxane, ethanol, 1-butanol, morpholine, and acetic acid were summarized in ref. 12 (Ooyama, Y.; Kumaoka, H.; Uwada, K.; Yoshida, K. *Tetrahedron* **2009**, *65*, 8336). Φ_s of PI-DPA in CHCl_3 solution was measured as 0.80 by using PI-DPA in ethanol ($\Phi_{\text{std}} = 0.82$) as the standard. Value of Φ_s can be calculated according to Eq. (1), where I_s and

I_{std} are the integrated emission intensities of the PI-DPA sample and the standard, respectively, A_s and A_{std} are the absorbance of the PI-DPA sample and the standard at the excitation wavelength, respectively, and η_s and η_{std} are the refractive indexes of the corresponding solutions (solvents).

$$\Phi_s = \Phi_{\text{std}} (I_s / A_s) (A_{\text{std}} / I_{\text{std}}) (\eta_s / \eta_{\text{std}})^2 \quad (1)$$

6. Fluorescence spectral change of CHO-TPA upon γ radiation

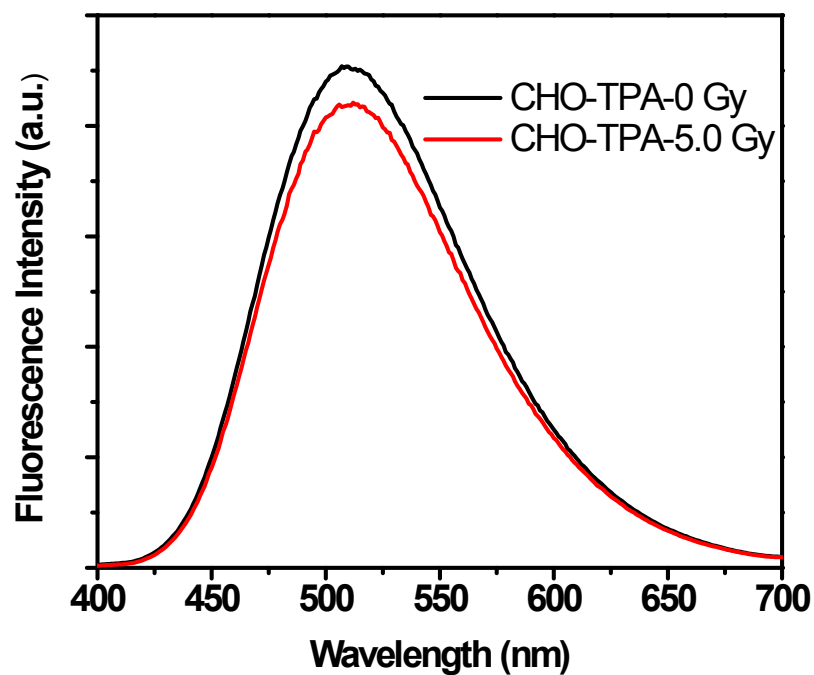


Figure S3. Fluorescence spectra of CHO-TPA (1×10^{-5} mol/L CHCl_3 solution) before and after exposure to 5 Gy of γ radiation.

7. Fluorescence spectral reversibility test of PI-DPA

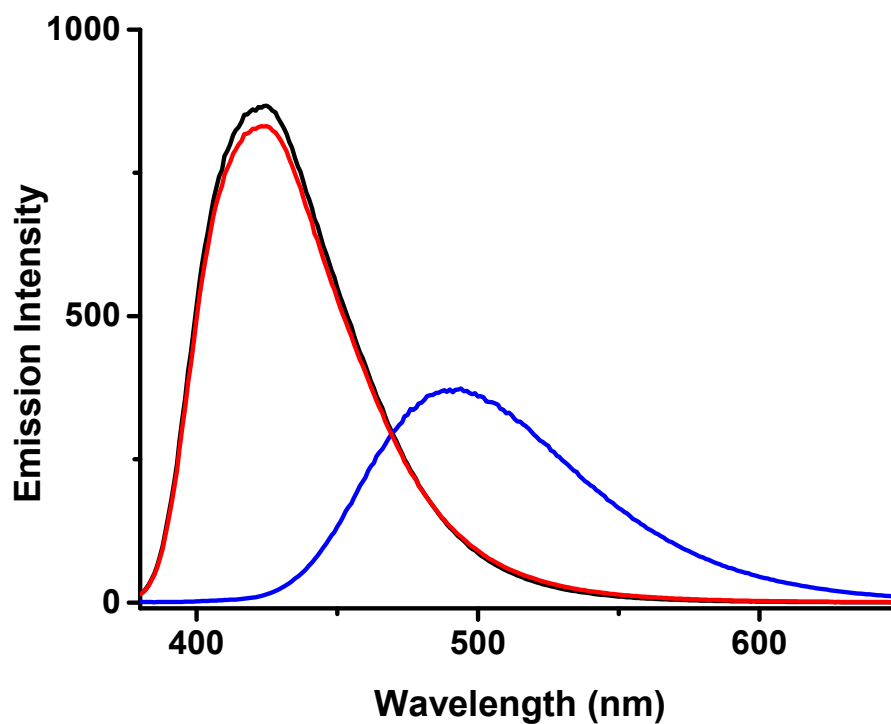


Figure S4. Fluorescence spectra of PI-DPA (1×10^{-5} mol/L CHCl_3 solution) before (black) and after (blue) 5 Gy of γ radiation. The fluorescence was recovered by addition of 1.5×10^{-4} mol/L triethylamine (red).

8. Fluorescence spectral comparison of PI-DPA in solutions and thin film

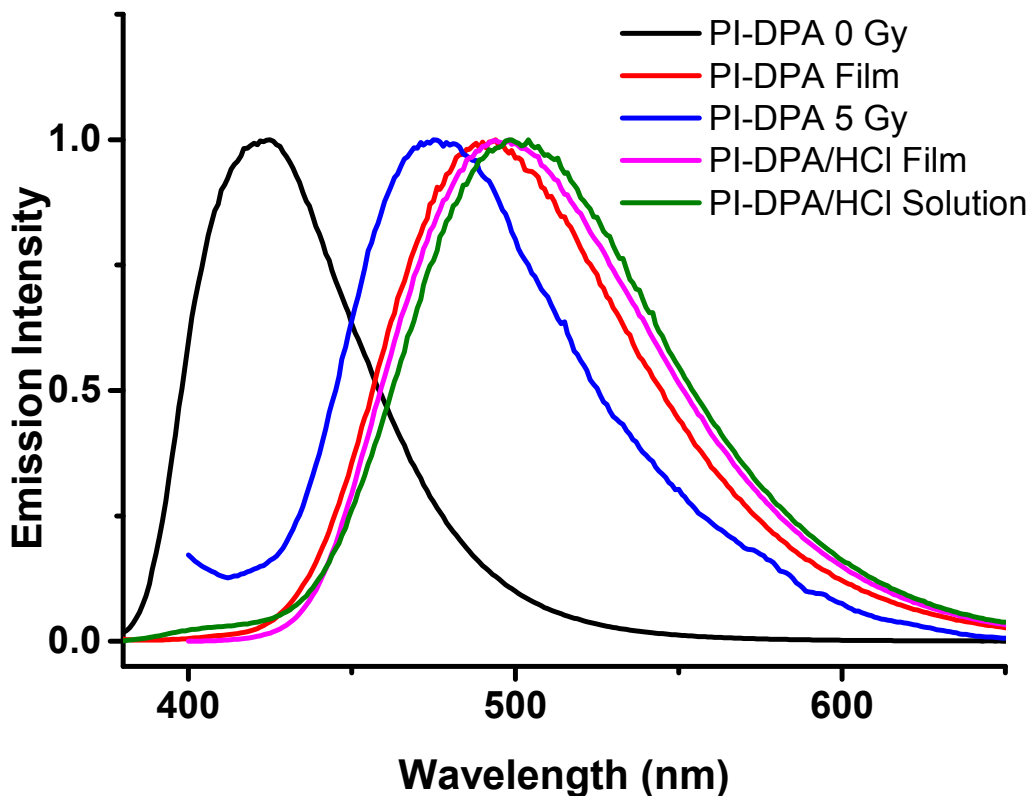


Figure S5. Normalized fluorescence spectra of PI-DPA solution (1×10^{-5} mol/L CHCl_3 solution) before (black) and after exposure to γ radiation (5 Gy, red), and the same solution after adding 1.4×10^{-5} mol/L HCl (paste from Figure 2d, green). Also shown are the normalized fluorescence spectra measured over the drop cast thin film of neutral PI-DPA (blue) and PI-DPA/HCl adduct (pink, drop cast from a solution with 20 times excess of HCl).

9. Spectral comparison of PI-DPA in DMSO solution upon HCl addition

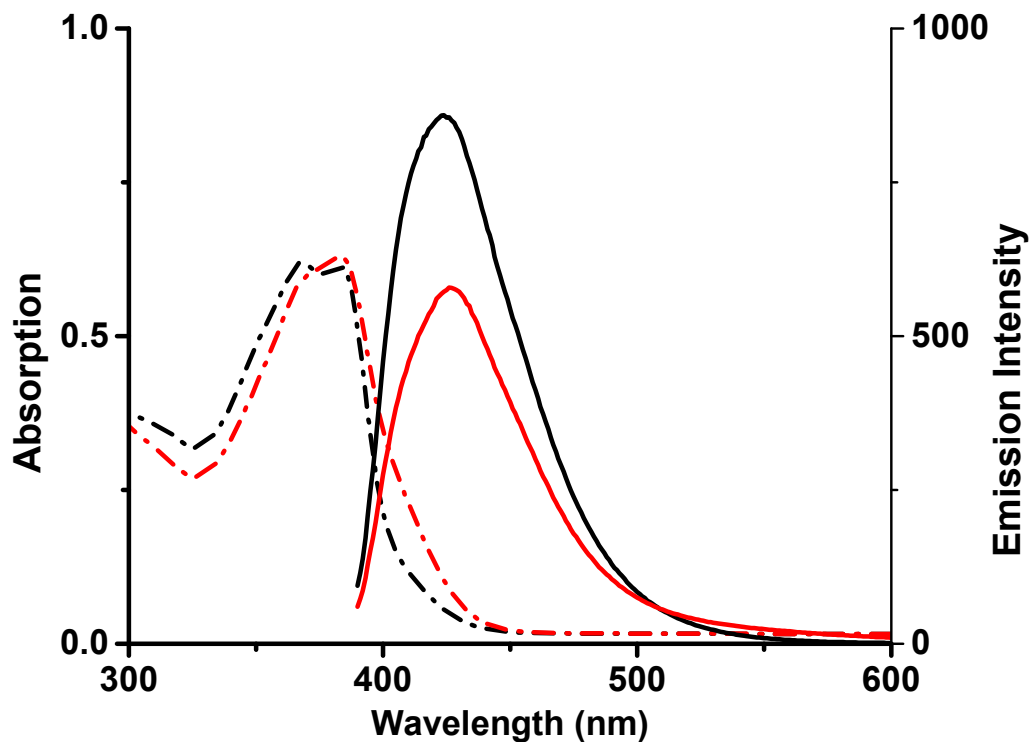


Figure S6. Absorption (dashed lines) and fluorescence (solid lines) spectra of PI-DPA in DMSO solution (1×10^{-5} mol/L) before (black) and after (red) adding HCl solution (1×10^{-4} mol/L). The excitation wavelength is 383 nm. As the protonated PI-DPA is soluble in DMSO, no aggregation was formed, though the fluorescence of protonated PI-DPA got slightly decreased.

10. Fluorescence spectral change of PI-DMA upon γ radiation

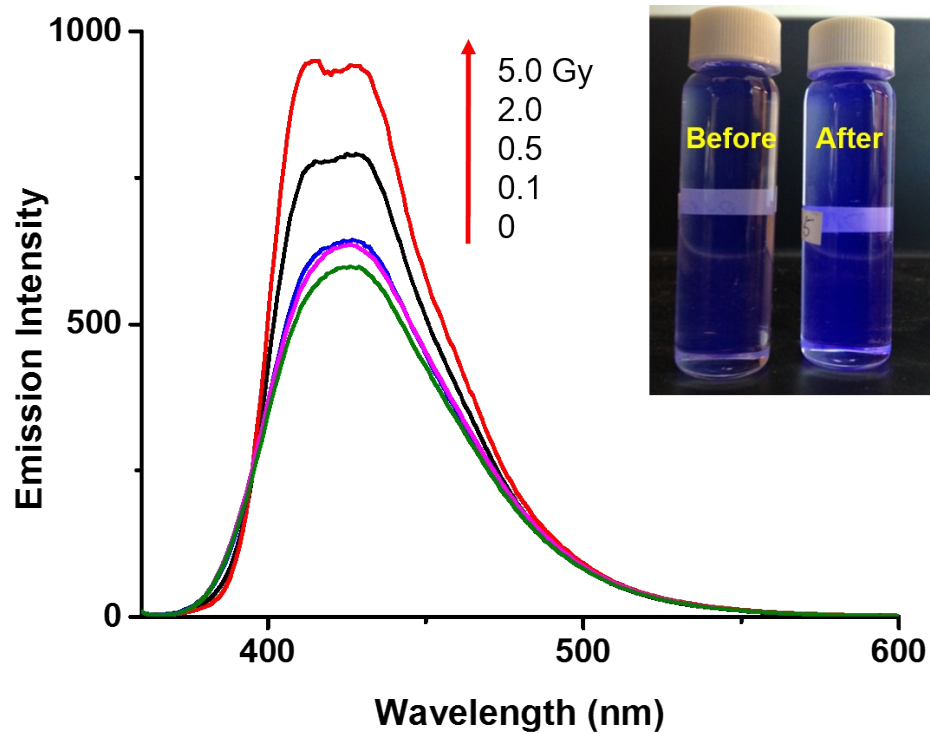


Figure S7. Fluorescence spectral change of PI-DMA (1×10^{-5} mol/L CHCl_3 solution) upon exposure to increasing dose of γ radiation. Also shown are the fluorescence photographs taken before and after exposure to 5 Gy of γ radiation.

11. Absorption and fluorescence spectral change of PI-DPA under γ , UV and sun light radiations

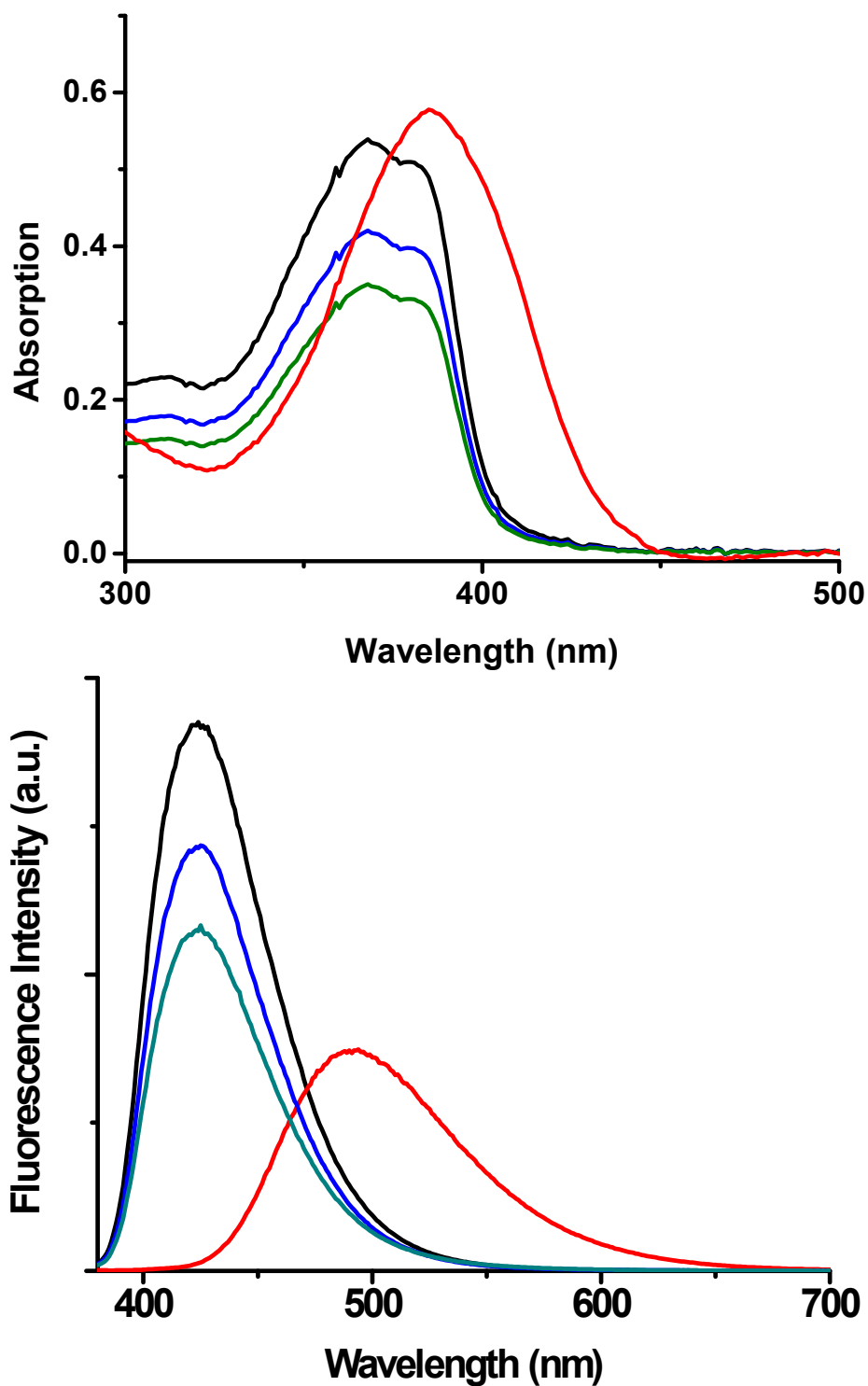


Figure S8. Absorption and fluorescence spectra of PI-DPA (1×10^{-5} mol/L CHCl_3 solution) before (black) and after exposure to 5 Gy of γ radiation (red), 1 h of UV light (254 nm, blue), and 24 h of sunlight (green).

12. ^1H NMR spectra of PI-DPA before and after binding with HAC

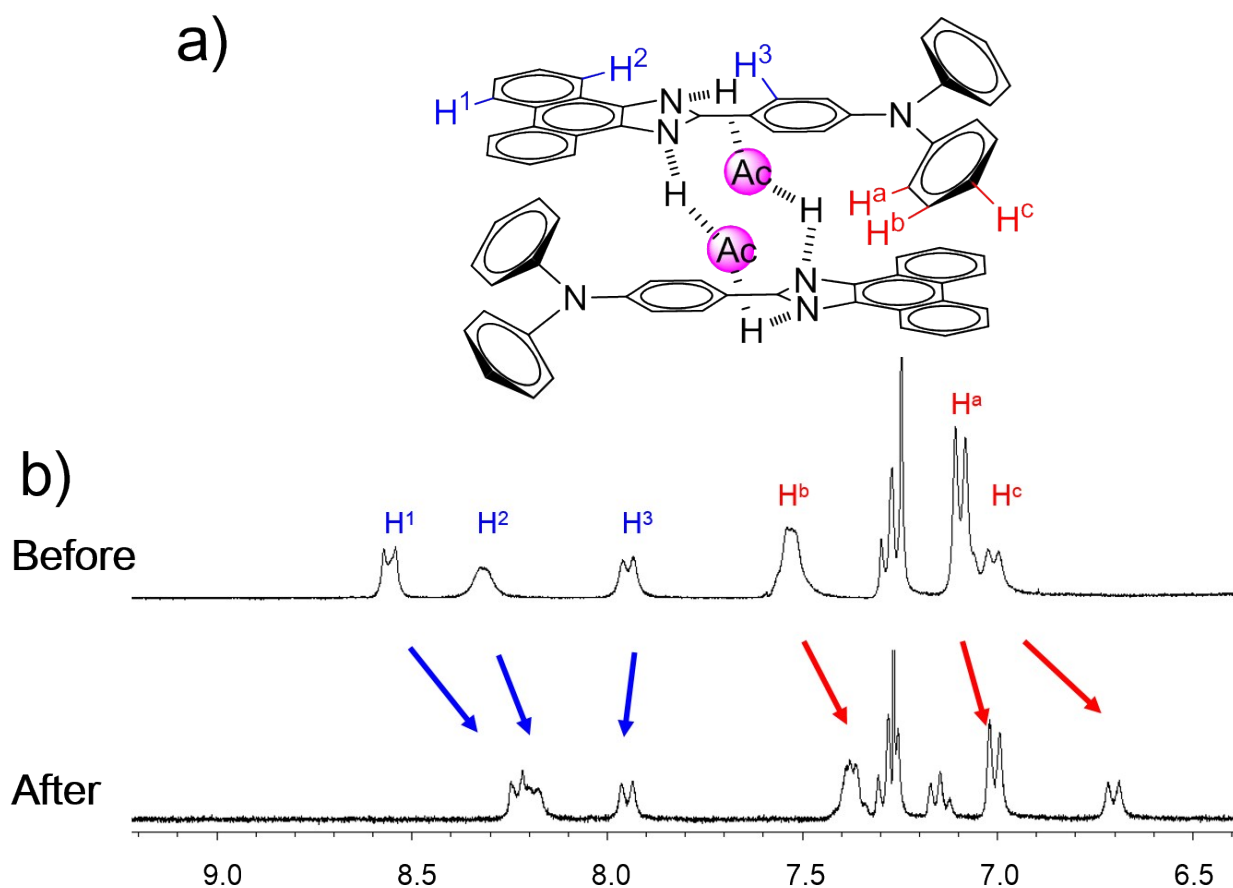


Figure S9. (a) Configuration of HAC assisted π - π stacking aggregation of PI-DPA molecules as revealed by the X-ray crystallography (ref. 12: Ooyama, Y.; Kumaoka, H.; Uwada, K.; Yoshida, K. *Tetrahedron* **2009**, 65, 8336); (b) Partial ^1H NMR spectra (CDCl_3) of PI-DPA (2 mmol) before and after the addition of HAC (20 mmol).

13. SEM image of drop cast film of neutral PI-DPA

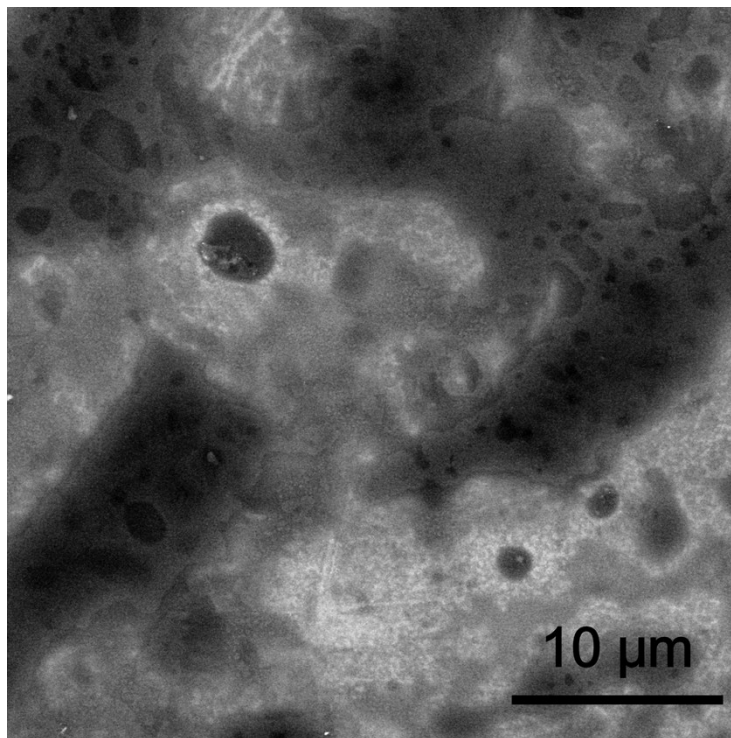


Figure S10. SEM image of the sample drop cast on silicon wafer from a neutral PI-DPA solution (1×10^{-5} mol/L in CH_2Cl_2).